Preprints (www.preprints.org) | NOT PEER-REVIEWED | Posted: 28 April 2023 doi:10.20944/preprints202304.1158.v1

Disclaimer/Publisher's Note: The statements, opinions, and data contained in all publications are solely those of the individual author(s) and contributor(s) and not of MDPI and/or the editor(s). MDPI and/or the editor(s) disclaim responsibility for any injury to people or property resulting from any ideas, methods, instructions, or products referred to in the content.

Article

Two-Color-Thermography For Temperature Determination In Laser Beam Welding Of Low-Melting Materials

Karen Schwarzkopf [1,2]*, Richard Rothfelder[1,2], Michael Rasch[1], Michael Schmidt [1,2]

[1] Institute of Photonic Technologies, Friedrich-Alexander-Universität Erlangen-Nürnberg, Konrad-Zuse-Str. 3/5, 91052 Erlangen, Germany

[2] Graduate School in Advanced Optical Technologies, Friedrich-Alexander-Universität Erlangen-Nürnberg, Paul-Gordan-Str. 6, 91052 Erlangen, Germany

* Correspondence: karen.schwarzkopf@lpt.uni-erlangen.de

Abstract: Knowledge of the temperature evolution is crucial to understand and control laser beam welding of low-melting materials. Existing temperature determination approaches are restricted to i) one-dimensional temperature information (e.g. ratio-pyrometers), ii) a priori knowledge of the emissivity (e.g. thermography) and iii) high temperature regions (e.g. two-wavelength imaging). In this paper, a ratio-based two-color-thermography approach is developed that allows for two-dimensional temperature determination in low-melting temperature ranges (< 1200 K). For static measurement situations it is demonstrated, that temperature can be determined despite variation in signal intensity and emissivity with high accuracy. The two-color-thermography set-up is further transferred into a commercial laser beam welding machine and experiments are conducted for varying process parameters. The direct application of the developed two-color-thermography system in dynamic process situations is limited as image artifacts presumably caused by internal reflections inside the optical beam path are present.

Keywords: two-color-thermography, temperature, temperature determination, ratio-based temperature measurement, laser beam welding, low-melting materials

1. Introduction

Laser beam welding of metals is a thermal driven joining process employing laser radiation as heat source. By focusing the laser radiation on top of the sample surface, the metal is – depending on the laser intensity – transferred from a solid to a liquid phase (conduction mode welding) and/or gaseous phase (keyhole mode welding) due to absorption by the material. Compared to conventional welding methods, laser beam welding is characterized by a narrow heat affected zone, increased processing speeds, and the ability to join a wide range of materials [1,2]. This is of high relevance e.g. in the automotive sector where joining of low-melting materials (such as die-casting aluminum (e.g. AlSi10MnMg) or aluminum wrought alloys (e.g. AlMg4,5Mn (AW5083), AlMgSi1 (AW6082)) is considered as major challenge due the associated hot cracking susceptibility.

Knowledge of the temperature evolution is crucial to understand and control microscopic and macroscopic process phenomena in laser beam welding of low-melting materials. On the microscopic process level, inadequate heat input can provoke strong heterogeneity of the microstructure (e.g. precipitation for Al-alloys) which in turn favors heterogeneity of the mechanical properties [3]. On the macroscopic process level, inadequate heat input can provoke an unstable melt pool behavior which in turn favors e.g. spatter formation, melt pool expulsion and porosity due to a collapsing keyhole [4]. Being able to determine spatial and temporal temperature information during the laser beam welding of low-melting materials is therefore fundamental to i) enhance process understanding, ii) increase process efficiency and iii) derive possible control approaches. In this paper, a ratio-based thermography method is presented for the first time that allows for spatially and temporally resolved temperature determination in low-melting temperature ranges (< 1200 K) despite variation in signal intensity and emissivity.

1.1 Temperature determination in laser beam welding

In laser beam welding mainly optical approaches are employed for temperature determination. While pyrometric methods generally provide pointwise (one-dimensional) temperature information, thermographic methods can also be used to determine temperature information with spatial (two-dimensional) resolution. Classical pyrometric or thermographic approaches depend on prior knowledge of the emissivity for correct temperature determination. The emissivity

© 2023 by the author(s). Distributed under a Creative Commons CC BY license.

Preprints (www.preprints.org) | NOT PEER-REVIEWED | Posted: 28 April 2023 doi:10.20944/preprints202304.1158.v1

ε is a dimensionless parameter that describes how well an object emits thermal radiation in comparison to an ideal black body radiator. The emissivity of an object depends on its material, temperature, phase, surface roughness, etc. and is only known to a limited extent [5]. Especially during laser material processing of metallic materials significant variations of emissivity can be present [6]. For instance, the emissivity of die casting iron is reported to vary between 0,45 (373 K) and 0,6 – 0,7 (1273 K) [7] and the emissivity for Inconel changes from 0,1 to 0,95 solely depending on the surface preparation [6]. Without the prior time-consuming experimental determination of the emissivity, only the so-called brightness temperature can be determined by means of classical pyrometry and thermography [8,9], which may not match the actual surface temperature with sufficient accuracy [5].

Ratio-based temperature determination methods are based on the collection of the emitted thermal energy in two closely spaced spectral ranges at the same time. Assuming that the intensity ratio of the detected spectral radiance changes constantly, temperature can be determined independently of local emission variations [10,11]. For a detailed explanation of the physical background the reader is referred to Chapter 2.1.1.

With two-color-pyrometry, a ratio-based, one-dimensional temperature determination method has already been established in laser material processing. Furumoto et al. record the surface temperature in a self-designed additive manufacturing setup using two-color pyrometry and demonstrate that the consolidation behavior of the powder particles depends on the introduced energy density [12]. Gutknecht et al. demonstrate under real process conditions that the signal from a two-color pyrometer correlates with the process stability [13]. Mitchell et al. demonstrate that there is a direct correlation between in-situ sensed temperature signatures and occurring porosity in the powder bed fusion process of metal alloys (PBF-LB/M) [14]. While ratio pyrometers allow sufficiently high temporal resolution of the melt pool temperature, they are not suitable for determining spatially resolved temperature information [15].

Two-color-thermography combines the advantages of two-color-pyrometry and thermography. Similar to the one-dimensional two-color-pyrometry approach, thermal radiation is separated into two narrow wavelength ranges but captured with a two-dimensional detector element instead, e.g. by identical camera sensors. By overlapping the signal intensity of individual detector elements congruently, the intensity ratio can be calculated pixel by pixel and temperature can be determined with spatial resolution despite local emissivity variations. To date, this approach has been used only sporadically in the context of laser material process. Hooper presents for the first time a coaxially guided two-color camera setup for temperature determination in the PBF-LB/M process for the purpose of process optimization [15]. The employed detector material is sensitive in a spectral range between 450 - 1000 nm, which corresponds to a temperature range between approx. 1000 - 4000 K. Due to a temporal and spatial highly resolved acquisition (acquisition rate: 100 kHz, spatial resolution: 20 µm) of surface temperatures on the melt pool level, varying temperature gradients can be recorded as a function of the process, geometry and position parameters for Ti6Al4V. However, due to limited memory capacities, the acquisition time is limited to 3 s, which limits the temperature acquisition to single layers. The coaxially guided two-color thermography system developed by Vallabh et al. allows the thermal radiation emitted from the process zone to be combined into a single camera sensor via two differently filtered beam paths [16]. The measurement system is characterized by an acquisition rate of 30 kHz at a spatial resolution of 20 µm and demonstrates for the first time that two-dimensional, ratio-based temperature acquisition can be implemented over multiple layers. The lowest temperature that can be detected by the system is reported to be 1300 K.

Currently, no measurement method is available that allows to determine spatial and temporal temperature information independent of local emissivity variations in laser material processing of low-melting metals (< 1200 K). As common materials such as AW5083 (T_{Melt} = 911 K) and AW6082 (T_{Melt} = 923 K) are susceptible to defect formation, recording of their thermal process behavior during laser beam welding is essential to further examine defect formation phenomena as well as to identify potential control approaches. For instance, laser beam welding of AW6082 is highly susceptible to hot cracking due to a low silicon and magnesium content (about 1 %). In contrast, laser-based welding of AW5083 has a reduced susceptibility to hot cracking due to a high magnesium content (about 4,5 %), but the high evaporation rate fosters process instabilities that lead to spatter formation, melt pool expulsion and porosity [4].

In this work, a temperature measurement set-up based on two-color-thermography is presented that allows to determine spatial and temporal temperature information below 1200 K independent of local emissivity variations. First, it is demonstrated that the experimental set-up allows stable temperature determination for static measurement situations despite variation in signal intensity and emissivity. Second, the two-color-thermography system is transferred into an industrial laser welding machine to investigate the ability of the temperature measurement set-up under dynamic process conditions for the first time.

The structure of this paper is as follows: in the material and methods chapter the physical background of the two-color-thermography approach and the system itself are presented. This is followed by the applied calibration and image

Preprints (www.preprints.org) | NOT PEER-REVIEWED | Posted: 28 April 2023 doi:10.20944/preprints202304.1158.v1

processing methods that enable the assignment of temperature values. Next, the methodology to demonstrate the stability of the two-color-thermography system towards signal intensity and emissivity changes are described and the integration into an industrial laser beam welding machine is stated. In the third chapter the results are presented followed by a discussion in the fourth chapter. The paper ends with a conclusion section that summarizes all findings and gives an outlook of future work approaches.

2. Materials and Methods

The following chapter is divided in five subsections. In the first section, the theoretical background of ratio-based temperature determination is explained. This is followed by the presentation and calibration of the developed two-color-thermography system. In the next section, the image processing steps are described to derive temperature information from individual images. Next, the methodology to prove the invariance of the two-color-thermography system towards signal intensity and emissivity changes is described followed by the last section that focuses on the integration and application of the two-color-thermography system into an industrial laser welding machine.

2.1 Two- color-thermography

2.1.1 Physical background

All objects with a temperature greater than absolute zero emit thermal radiation. The spectral radiance M ($W \cdot sr^{-1} \cdot m^{-3}$) that is emitted by an ideal black body for wavelength λ at absolute temperature T is given by Planck's radiation law:

$$M_\lambda(\lambda, T) = \frac{2\pi hc^2}{\lambda^5} \cdot \frac{1}{e^{\frac{hc}{\lambda k_B T}} - 1} \tag{1}$$

where h is the Planck constant, c is the speed of light, and k_B is the Boltzmann constant. With an increase in temperature the absolute amount of emitted energy of an object increases while the peak of the emitted spectrum shifts to smaller wavelengths.

Real objects do not emit thermal radiation perfectly. To describe how well an object emits thermal radiation in comparison to an ideal black body radiator the dimensionless parameter emissivity ε is introduced. The emissivity of an object depends on its material, temperature, phase, surface roughness, etc. and is only known to a limited extent [5]. Especially during laser material processing of metallic materials significant variations of emissivity can be present [6]. These process-induced emissivity variations hinder the direct application of Planck's law for temperature determination based on a single wavelength in laser material processing. One approach to overcome this limitation is by simultaneous measure the spectral radiance at two narrow but separated spectral bands.

By measuring the thermal radiation of an object within two spectral bands ($\lambda_{1,min} - \lambda_{1,max}$, $\lambda_{2,min} - \lambda_{2,max}$), two signal intensities I_1 and I_2 are determined and the following intensity ratio r can be determined:

$$r = \frac{I_1}{I_2} = \frac{\int_{\lambda 1,min}^{\lambda 1,max} \eta_1 \cdot \varepsilon_1(\lambda_1, T) \cdot M_{\lambda,1}(\lambda_1, T) \cdot d\,\lambda}{\int_{\lambda 2,max}^{\lambda 2,max} \eta_2 \cdot \varepsilon_2(\lambda_2, T) \cdot M_{\lambda,2}(\lambda_2, T) \cdot d\lambda} \tag{2}$$

where η is the combined efficiency of the optical path and the quantum efficiency of the detector (here: based on indium gallium arsenide (InGaAs)). Under the assumption that the chosen wavelength regions are close to each other and that the relative change of the emissivity is constant it can be assumed that $\varepsilon_1 \sim \varepsilon_2$. Then, the formula can be noted as follows:

$$r = \frac{I_1}{I_2} = \frac{\int_{\lambda 1,min}^{\lambda 1,max} \eta_1 \cdot M_{\lambda,1}(\lambda_1, T) \cdot d\,\lambda}{\int_{\lambda 2,max}^{\lambda 2,max} \eta_2 \cdot M_{\lambda,2}(\lambda_2, T) \cdot d\lambda} \tag{3}$$

If the change in emissivity affects both spectral ranges to the same extent, temperature can be determined eliminating any error from emissivity variation [6]. Under the gray body assumption, an emissivity-independent expression of temperature T can be noted:

$$T = \frac{k_B \cdot (\lambda_1 - \lambda_2)}{\lambda_1 \cdot \lambda_1 \cdot ln\,(r \cdot \frac{\lambda_2}{\lambda_2})^5} \tag{4}$$

Preprints (www.preprints.org) | NOT PEER-REVIEWED | Posted: 28 April 2023 doi:10.20944/preprints202304.1158.v1

2.1.2 Experimental Set-Up And Combined Optical Path Efficiency

The two-color-thermography set-up combines two identical InGaAs-sensors (C15370-01, Hamamatsu Photonics Deutschland GmbH) with an optical lens and filter system, as shown in Fig. 1a. All optical elements are attached to a customized mounting plate in order to enable lateral integration of the measurement set-up into an industrial laser welding machine. The thermal radiation from the laser welding process zone is directed via an achromat (f = 250 mm, AC508-250-C-ML, Thorlabs) onto a dichroic beamsplitter (HR1030-1070HT800-1700, Laser Components). Due to a customized optical coating, the dichroic beamsplitter is on the forefront highly reflective in the wavelength range between 1350 nm – 1580 nm (beam path 1) and highly transmissive between 1620 nm – 1800 nm (beam path 2). The backfront of the dichroic mirror is coated with an additional anti-reflection coating minimizing reflectivity to < 1 %. After passing the spectral partition stage, the wavelengths of interest pass a second achromat (f = 250 mm, AC508-250-C-ML, Thorlabs) in each of the individual beam paths. In the final step, the thermal radiation is focused on the respective camera sensor by a lens (LF1547-C, Thorlabs). The simulated combined efficiency (multiplication of the optical path and the detector efficiency) is plotted against the wavelength for beam path 1 (blue) and beam path 2 (orange) in Fig. 1b. For both beam paths the combined efficiency is greater than 72 % in the wavelength region of interest (gray). The employed InGaAs-sensors for temperature analysis allow recording speeds of up to 507 frames per second at a resolution of 320 x 256 pxl² with a 16 bit pixel depth. To reduce the thermal noise, the InGaAs-sensors are constantly cooled to a temperature of 253 K during operation.

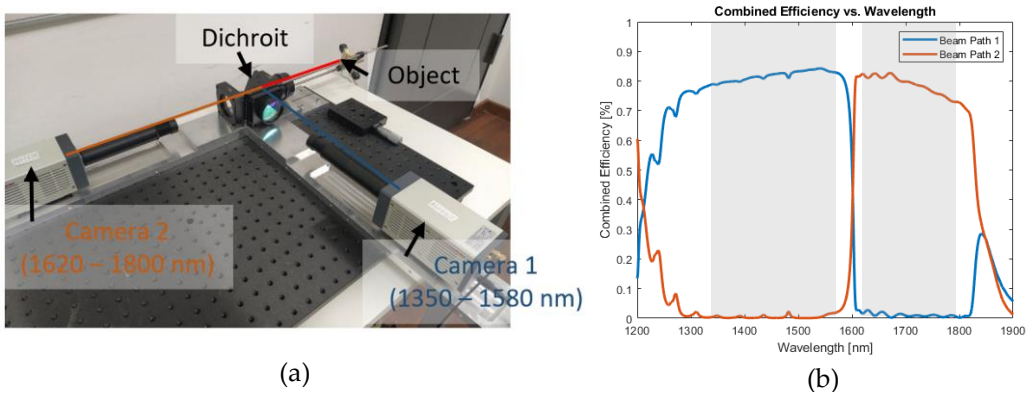

(a) (b)

Figure 1. (a) Experimental set-up of the two-color-thermography set-up. The system employs two identical but spectrally differently filtered InGaAs-sensor modules (C15370-01, Hamamatsu Photonics Deutschland GmbH). (b) Simulated combined efficiency along the two spectral differently filtered beam paths (blue: beam path 1 (spectral band: 1350 - 1580 nm), red: beam path 2 (spectral band: 1620 - 1800 nm)) plotted against the wavelength.

2.2 Calibration

To correlate the ratio of the signal intensities with temperature, a calibration measurement based on a blackbody radiation source is conducted. The blackbody radiation system (Pegasus R Model 970, Isothermal Technology Ltd.) is housed – with suitable insulation – into a tube furnace. The cavity of the tube furnace measures 65 mm in depth, 20 mm in diameter, and its emissivity is specified with 0,995 [17]. The temperature of the furnace is set via a control panel, while the actual radiation temperature is measured by a thermocouple that is additionally inserted into the cavity. The temperature range of the blackbody radiation lies between 423 K – 1473 K. To collect the signal intensity of the individual camera sensors at a defined temperature, the two-color-thermography system is coaxially aligned to the cavity aperture of the black body radiator system. The focal plane of the system is positioned approx. in the middle of the cavity depth. A calibration curve ranging between 473 K – 1450 K (step size = 50 K) is derived. At each temperature plateau, the signal intensity is determined by averaging the signal intensity values of 50 consecutive frames for both camera sensors. In Fig. 2 , the determined calibration curves plots the intensity ratio versus the temperature. The experimentally determined data points (black stars) have a linear slope that can be approximated by the following linear equation (red line)

$$T = 1391 \cdot r - 145 \quad (4)$$

where T is temperature and R is the intensity ratio.

Preprints (www.preprints.org) | NOT PEER-REVIEWED | Posted: 28 April 2023 doi:10.20944/preprints202304.1158.v1

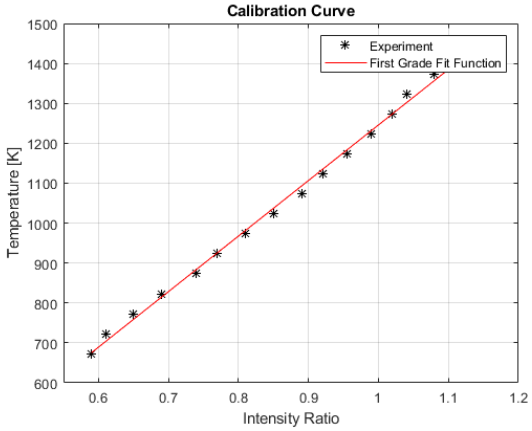

Figure 2. Calibration curve of the two-color-thermography system plotting the intensity ratio versus temperature. The slope of the experimentally determined data points can be approximated by the following linear equation: $T = 1391 \cdot r - 145$.

2.3. Image Processing

In this section it is explained how temperature information is extracted from individual images. It shall be noted that all experiments presented in this paper are employing the full sensor area (320 x 260 pxl²) and the maximal frame rate of 507 fps. Fig. 3 visualizes the five image processing steps that are applied:

1. Initial raw images:
   $I_{1,Roh}(x,y)$, $I_{2,Roh}(x,y)$
2. Subtraction of dark-frame images from raw images:
   $I_{1,Roh}(x,y) - I_{1,Korr}(x,y)$, $I_{2,Roh}(x,y) - I_{2,Korr}(x,y)$
3. Noise-corrected images (elimination of dark current and fixed-pattern noise):
   $I_1(x,y)$, $I_2(x,y)$
4. Image alignment based on similarity measure (cross-correlation)

Calculation of intensity ratio and temperature assignment for each pixel.

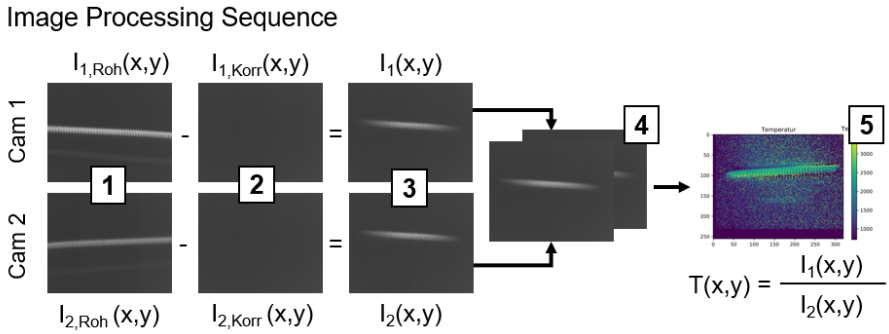

Figure 3. Exemplary sequence of image processing steps for temperature determination with the two-color-thermography system. (1) raw images, (2) dark-frame images, (3) noise-corrected images, (4) image alignment, (5) calculation of intensity ratio and temperature assignment.

2.4 Proof-of-Concept

To prove the working principle of the developed two-color-thermography system, two research hypothesis are formulated. The first hypothesis states, that a variation of the signal intensity (energy that is collected by the camera sensors) does not affect the temperature determination based on the two-color-thermography system. The second hypothesis states, that a variation of emissivity does not affect the temperature determination based on the two-color-thermography system. Both research hypothesis shall be tested for static process situations, meaning that the thermal emitter is not moving.

Preprints (www.preprints.org) | NOT PEER-REVIEWED | Posted: 28 April 2023 doi:10.20944/preprints202304.1158.v1

The first research hypothesis is tested by varying the exposure time of the two camera sensors while keeping the emitted thermal energy constant. An increase of the exposure time leads to an increase of thermal radiation that is collected by the InGaAs-sensors. The thermal radiation is emitted by the same black body radiator system that is used for the calibration. The target temperature is set to 1173 K. Two exposure times (5 µs and 10 µs) are compared. It is expected that the calculated mean temperature is constant despite changing the exposure time.

To test the second research hypothesis a metallic checkerboard (8 x 9 tiles) with edge length of 250 µm is used. In Fig. 4 the custom-made checkerboard is shown from the top-view perspective. Some of the tiles of the checkerboard are laser-marked changing their surface structure in such a way that they appear darker compared to the unmarked tiles. The change of surface appearance comes with a change in emissivity resulting in a metal surface with varying emissivity properties. To test the second research hypothesis, the checkerboard is placed on a heating plate and heated over a wide range of temperatures. The temperature of the heating plate is manually set. The pre-set temperature is internally measured and displayed on a control screen. As the unmarked and laser-marked tiles have different emissivity properties, the intensity of the thermal radiation directed towards the InGaAs-sensors is expected to vary. According to the second research hypothesis it is expected that the calculated mean temperature is constant despite emissivity variation.

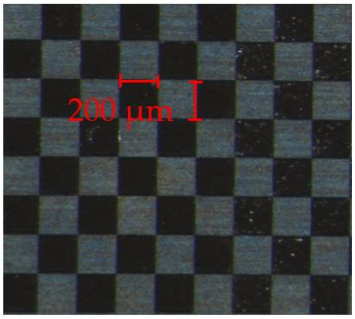

Figure 4. Top-view of a laser-marked checkerboard that is used to prove, that the two-color-thermography system is insensitive to emissivity changes. The emissivity of the dark and bright tiles differs.

2.5 Experimental Set-Up For Laser Beam Welding

To investigate the ability of the developed two-color-thermography system in dynamic process situations, the experimental set-up is integrated into an industrial laser welding and cutting machine (ERLASER UNIVERSAL, Erlas GmbH). By means of the two-color-thermography set-up, it is aimed to identify temperature-related process characteristics (e.g. cooling rate, thermal gradient) and correlate them with the process result (e.g. melt pool depth and width). The industrial laser beam welding system including the thermal imaging system is shown in Fig. 5. The laser beam welding machine consists of an enclosed housing that contains the work area, a welding scanner unit and a TruDisk 8001 (λ = 1.030 nm) disk laser with a maximum output power of 8 kW. The laser beam is focused through the processing optics onto the surface of a metal sheet (50 x 100 x 5 mm³, AW5083) and guided along the x-axis along the workpiece. The focus diameter is approx. 100 µm. The laser power and the scan velocity are varied between 200 W and 500 W and 100 mm/s and 500 mm/s respectively. The two-color-thermography system is laterally focused on the workpiece with an inclination of approx. 41°. The exposure time of the InGaAs-cameras is set to 1 µs. The two-color-thermography set-up is manually triggered before and after the laser radiation is emitted.

Preprints (www.preprints.org) | NOT PEER-REVIEWED | Posted: 28 April 2023 doi:10.20944/preprints202304.1158.v1

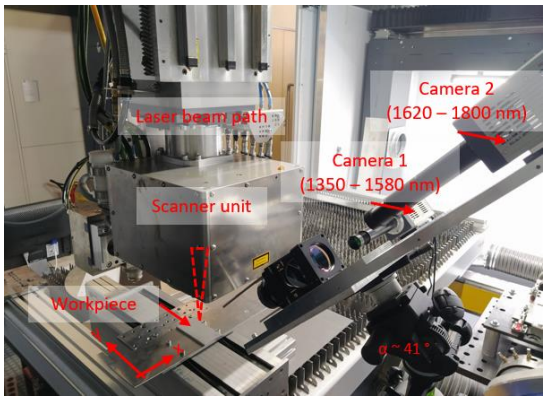

Figure 5. Off-axis integration of the two-color-thermography set-up into the industrial laser welding machine. The laser beam is guided in x-direction across the work piece with a scanner unit. The laser-matter-interaction zone is simultaneously observed with the two-color-thermography set-up. The set-up is inclined by approx. 41° relative to the work piece surface.

3. Results

This chapter is divided in two subsections. The first section presents the experimental results of the static measurement situation, where it is proved that temperature determination by means of the two-color-thermography system is insensitive to changes in signal intensity and emissivity. In the second section, the findings from the laser beam welding experiments with a commercial laser beam welding machine are presented.

3.1. Static measurement situation

3.1.1 Influence of signal intensity on temperature determination

In this section the results of the examination of the first research hypothesis are presented. The first hypothesis states, that a variation of the signal intensity (energy that is collected by the camera sensors) does not affect the temperature determination based on the two-color-thermography system. In Fig. 6 the two thermograms are compared against the defined temperature of 1173 K. On the left side (Fig 6a) the spatial temperature distribution for the lower exposure time of 5 µs is plotted against the full sensor area (320 x 260 pxl²). The thermogram on the right side (Fig. 6b) shows the spatial temperature istribution for doubled exposure time of 10 µs.

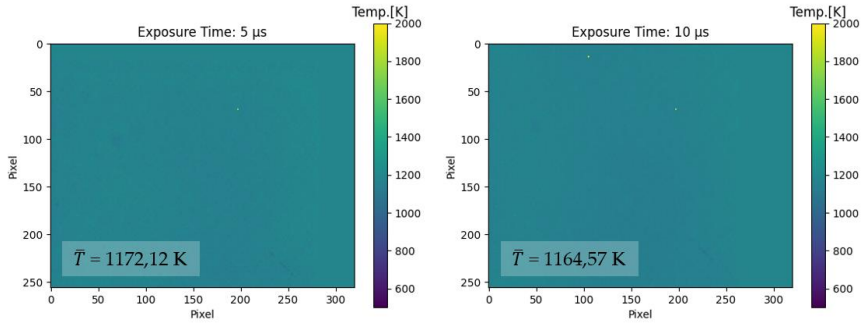

(a) (b)

Figure 6. Influence of signal intensity on temperature determination by varying exposure time. The temperature is set to 1173 K while the exposure time is changed from (a) t_{exp} = 5 µs to (b) t_{exp} = 10 µs. Despite varying the signal intensity, temperature values can be determined with high accuracy (deviation < 0,001 % for 5 µs and -0,007 % for 10 µs).

The determined mean temperature is 1172,12 K for the lower exposure time (5 µs) and 1164,57 K for the higher exposure time (10 µs). The resulting mean temperature value differ from the defined temperature of 1173 K by less than 0,001 % (1172,12 K / 1173 K) for the experiment with the low exposure time and by -0,007 % (1164,57 K / 1173 K) for the higher exposure time respectively. The temperature deviation from the defined temperature is comparably low for both

Preprints (www.preprints.org) | NOT PEER-REVIEWED | Posted: 28 April 2023 doi:10.20944/preprints202304.1158.v1

examined exposure times. In comparison, the measurement accuracy of commercially available thermography devices is stated with ± 1 %). It shall be noted that the determined temperature is based on an average value, and a comparison with commercially available device must be regarded with caution at this development state of the set-up. Nevertheless, it is demonstrated that the two-color-thermography system is able to determine temperature values with high accuracy and independent of the signal intensity. The first research hypothesis is thus confirmed. It is concluded that temperature determination based on the two-color-thermography system is insensitive to process-induced intensity fluctuations caused by e.g. contaminated protective glasses.

3.1.2 Influence of emissivity variation on temperature determination

In this section the results of the examination of the second research hypothesis are presented. The second hypothesis states, that a variation in emissivity does not affect the temperature determination based on the two-color-thermography system. Fig. 7 consists of three subplots that illustrate the two raw images from the differently filtered spectral ranges (Camera 1, 1350 – 1580 nm (Fig. 7a) and Camera 2, 1620 – 1800 nm (Fig. 7b)) and the resulting thermogram (Fig. 7c) for the given temperature of 798 K.

For the raw images, the signal intensity is plotted against the full sensor area. In both images, the checkerboard and its individual tiles with varying emissivity (laser-marked: bright tiles, unmarked: dark tiles) are visible. It can be noted, that for the spectral region comprising smaller wavelengths (Fig. 7a) the signal intensity is globally viewed lower (or: darker) compared to the spectral region comprising the higher wavelengths (Fig. 7b). This is based on Planck's radiation law, where the emitted spectral radiance at the given temperature of 798 K is lower for the smaller wavelength band. Therefore, less energy is collected by the sensor of Camera 1 resulting in a less bright appearance of the checkerboard. Based on the prior described image processing sequence, the two raw images are processed, resulting in the plotted thermogram (Fig. 7c). Unlike the raw images, the checkerboard is not visually distinguishable within the thermogram. This also manifests in the determined mean temperature of the thermogram that is 806,29 K. The mean temperature deviates from the defined temperature by 0,01 % (806,29 K / 798 K). This proves that the two-color-thermography set-up is able to determine temperature values with high accuracy despite variation of emissivity. Thus, also the second research hypothesis is also confirmed.

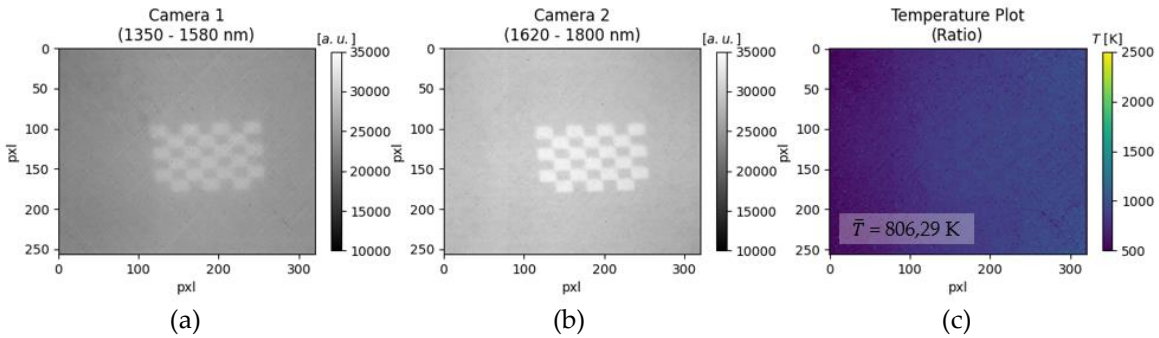

Figure 7. Influence of emissivity on temperature determination. A checkerboard is placed on a heating plate and heated to 798 K. The thermal radiation emitted by the unmarked and laser-marked tiles differs leading to a lower signal intensity for the unmarked and a higher signal intensity for the laser-marked regions. The checkerboard is observed with Camera 1 (a) and Camera 2 (b). The mean temperature (806,29 K) of the processed ratio-image deviates less than 0,01 % from the defined temperature (798 K).

Since both research hypothesis are confirmed as true, it is proved that the presented two-color-thermography approach is a legitimate method for temperature determination despite variation of signal intensity and variation of emissivity. In both experiments, the deviation from the defined temperature is below 0,01 %. In the next section, the results of the experimental trials with the two-color-thermography set-up in an industrial laser beam welding machine are presented.

Preprints (www.preprints.org) | NOT PEER-REVIEWED | Posted: 28 April 2023 doi:10.20944/preprints202304.1158.v1

3.2. Dynamic measurement situation

In this section, the results of the experimental trials in the commercial laser beam welding machine are presented. The main goal was to investigate the ability of the developed two-color-thermography system in dynamic process situations. Based on the two-color-thermography set-up, it is aimed to identify temperature-related process characteristics (e.g. cooling rate, thermal gradient) and correlate them with the process result (e.g. melt pool depth and width).

During all experiments with the industrial laser beam welding machine, a characteristic image artifact is present. An exemplary visualization is shown in in Fig. 8a and 8b for experiments with a laser power of 200 W and a scan velocity of 100 mm/s. In both spectral bands, a duplicate of the actual scene (here: laser-material interaction zone) is overlaid upon the desired image. However, it is physically impossible to have two laser-material interaction zones emitting towards the camera sensors, as only one laser beam source was used during the trials.

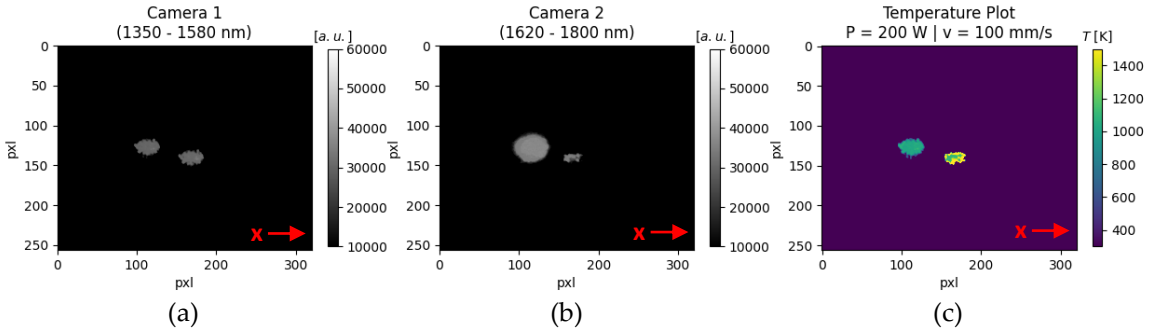

Figure 8. Image artifact during laser beam welding trials (P = 200 W and v = 100 mm/s) in an industrial laser beam welding machine. In both spectral regions, a duplicate of the actual laser-material interaction zone is present.

Temperature determination under these circumstances is barely possible. First it remains unclear which of the laser-material interaction zone is the original and which the duplicate. Since the length (elongation along the x-direction) of the upper left object displayed in the thermogram (Fig. 8c) is in conformity with the expected melt pool length (approx. 500 µm) for the chosen process parameters, it is concluded that this is the original laser-material interaction zone. Therefore, the right object in the resulting thermogram is not valid and will not be considered. The mean temperature of the right object is approx. 1000 K. From a physically perspective this is reasonable, as the temperature value ranges between the melting (911 K) and evaporation (1883 K) temperature of the investigated AW5083 material. However, there is no temperature variation notable between the center and the contours. A constant temperature evolution within the melt pool is doubtful, as a temperature decline from the center of the melt pool towards the edges is expected.

4. Discussion

4.1. Static process situation

With the developed two-color-thermography set-up temperature could be determined for static measurement objects with high accuracy despite variation in i) signal intensity and ii) emissivity. Having the ability to temporally and spatially determine temperature independent of changes in signal intensity is of great benefit in laser beam welding. For instance, contaminated protective glasses or process fumes attenuate the signal that is directed towards the sensor unit. Measurement methods (e.g. pyrometer, thermography) that are not able to account for such signal attenuations, will determine temperature values that are strongly deviating from the defined temperature value leading to wrong process assumptions. Especially the ability of the presented two-color-thermography system to measure the temperature evolution with high temporal and spatial resolution despite emissivity changes is a huge potential for laser material processing. As stated before, emissivity can change drastically for commonly used materials in laser-based manufacturing processes [6]. Having a tool that is able to determine temperature reliably despite emissivity changes is therefore of high relevance.

Preprints (www.preprints.org) | NOT PEER-REVIEWED | Posted: 28 April 2023 doi:10.20944/preprints202304.1158.v1

4.2. Dynamic process situation

The two-color-thermography set-up was successfully transferred into an industrial laser beam welding machine to investigate its ability to measure temperature in a dynamic process situation. However, temperature determination during laser beam welding is only possible to a very limited extend with the current set-up. Image artifacts in form of duplicates of the laser-material interaction zone are present during all conducted process parameter sets. The occurring duplicates can be explained by the ghost imaging phenomena. The reason for this are internal (multi-) reflections from surfaces within the beam path [18]. Possible sources of error could be e.g a misalignment of optical components or reflections caused at the backside of the dichroic mirror. Although the back of the dichroic mirror is coated with a special anti-reflection coating, in average up to 1 % of the incident light could be reflected. This might be unfavorable for dynamic process situations but further investigations are necessary and an optimization of the optical beam path design is intended.

An alternative design approach could be based on optical components that are known to eliminate ghosting phenomena e.g. pellicle beamsplitters. A pellicle is an ultra-lightweight membrane that virtually eliminates multiple reflections due to extreme thinness of the membrane. Unlike for thicker beam splitters made of glass, the secondary reflections are eliminated by making them coincident with the original beam. However, the extreme thinness of the pellicle makes it very fragile and caution is required when using them.

5. Conclusions

The main conclusions from the conducted investigations are summarized in the following:

1. A temperature determination set-up based on the ratio-principle was presented. Unlike existing ratio-principle approaches, the developed with the two-color-thermography set-up is designed for temperature regions for low-melting materials (< 1200 K) based on InGaAs-sensors.
2. It was demonstrated for static measurement situations, that temperature determination is possible despite variation in signal intensity with the two-color-thermography system. For two different exposure times, the resulting mean temperature differed by < 0,007 % from the defined temperature value.
3. For static measurement tasks it was shown, that temperature determination is possible despite variation of emissivity with the two-color-thermography system. Employing a custom-made checkerboard with tiles of different emissivity, the mean temperature deviated by less than 0,01 % from the defined temperature value.
4. Image artifacts presumably caused by internal reflections inside the optical path of the two-color-thermography system restrict the direct transition of the set-up into a commercial laser welding machine.
5. Further investigations and optimization of the optical beam path design will be conducted to allow for reliable temperature measurement during laser beam welding of low-melting materials.

Author Contributions: Conceptualization, Karen Schwarzkopf; methodology, Karen Schwarzkopf; software, Karen Schwarzkopf; validation, Karen Schwarzkopf; data curation, Karen Schwarzkopf; writing—original draft preparation, Karen Schwarzkopf.; writing—review and editing, Karen Schwarzkopf, Richard Rothfelder and Michael Schmidt; visualization, Karen Schwarzkopf; supervision, Michael Schmidt; funding acquisition, Michael Rasch and Michael Schmidt. All authors have read and agreed to the published version of the manuscript.

Funding: The authors acknowledge financial support by the Deutsche Forschungsgemeinschaft (DFG, German Research Foundation) for grant number 280377472 as well as the financial support for the collaborative research center 814 subproject A5 and transfer project T8. Additionally, the authors acknowledge financial support of the Erlangen Graduate School in Advanced Optical Technologies (SAOT) by the Bavarian State Ministry for Science and Art.

Preprints (www.preprints.org) | NOT PEER-REVIEWED | Posted: 28 April 2023 doi:10.20944/preprints202304.1158.v1

Data Availability Statement: The data presented in this study are available on request from the corresponding author.

Acknowledgments: The authors would like to thank Mr. Jürgen Gottlieb for his technical support during the laser welding trials.

Conflicts of Interest: The authors declare no conflict of interest.

References

1. Sokolov, M. and Salminen, A. Improving Laser Beam Welding Efficiency. Engineering 2014, vol. 6, pp. 559-571. doi: 10.4236/eng.2014.69057.
2. Svenungsson, J.; Choquet, I.; Kaplan, A. Laser Welding Process – A Review of Keyhole Welding Modelling. Physics Procedia 2015, pp. 182–191.
3. Hakem, M.; Lebaili, S.; Mathieu, S.; Miroud, D.; Lebaili, A.; Cheniti, B. Effect of microstructure and precipitation phenomena on the mechanical behavior of AA6061-T6 aluminum alloy weld. The International Journal of Advanced Manufacturing Technology 2019, vol. 102, pp. 2907–2918. https://link.springer.com/content/pdf/10.1007/s00170-019-03401-1.pdf?pdf=button
4. Gref, W. Laserstrahlschweißen von Aluminiumwerkstoffen mit der Fokusmatrixtechnik. Dissertation, Stuttgart, Univ. 2015. ISBN 3-8316-0537-8.
5. Mohr, G.; Nowakowski, S.; Altenburg, S. J.; Maierhofer, C.; Hilgenberg, K. Experimental Determination of the Emissivity of Powder Layers and Bulk Material in Laser Powder Bed Fusion Using Infrared Thermography and Thermocouples. Metals 2020, vol. 10, no. 11, pp. 1546, doi: 10.3390/met10111546.
6. Davies, M. A.; Ueda, T.; M'Saoubi, R.; Mullany, B.; Cooke, A. L. On The Measurement of Temperature in Material Removal Processes. CIRP Annals 2007, vol. 56, no. 2, pp. 581-604. doi: 10.1016/j.cirp.2007.10.009.
7. Novasens Sensortechnik Heuer. Emissionsgradtabelle für die Infrarot Temperaturmessung. [online]. https://www.novasens.de/wp-content/uploads/Emissionsgradtabellenovasens.pdf (Accessed April 11, 2023).
8. Pavlov, M.; Doubenskaia, M.; Smurov, I. Pyrometric analysis of thermal processes in SLM technology. Physics Procedia 2010, vol. 5, pp. 523–531. doi: 10.1016/j.phpro.2010.08.080.
9. Heigel, J. and Lane, B. The effect of powder on cooling rate and melt pool length measurements using in situ thermographic techniques, Proceedings of the Solid Freeform Fabrication Symposium 2017, Austin, TX, [online]. https://tsapps.nist.gov/publication/get_pdf.cfm?pub_id=923988 (Accessed April 11, 2023).
10. Herman, I.P. Optical diagnostics for thin film processing: Chapter 13 - Pyrometry. Academic Press 1996, San. Diego, Calif., USA.
11. Müller, B.; Renz, U. Development of a fast fiber-optic two-color pyrometer for the temperature measurement of surfaces with varying emissivities. Review of Scientific Instruments 2001, vol. 72, no. 8, pp. 3366–3374, doi: 10.1063/1.1384448.
12. Furumoto, T.; Ueda, T.; Alkahari, M; Hosokawa, A. Investigation of laser consolidation process for metal powder by two-color pyrometer and high-speed video camera. CIRP Annals 2013, vol. 62, no. 1, pp. 223–226, doi: 10.1016/j.cirp.2013.03.032.
13. Gutknecht, K.; Haferkamp, L.; Cloots, M.; Wegener, K. Determining process stability of Laser Powder Bed Fusion using pyrometry. Procedia CIRP 2020, pp: 127 – 132, doi: 10.1016/j.procir.2020.01.147.
14. Mitchell, J.; Ivanoff, T.; Dagel, D.; Madison, J.; Jared, B. Linking pyrometry to porosity in additively manufactured metals. Additive Manufacturing 2020, vol. 31, p. 100946, doi: 10.1016/j.addma.2019.100946.
15. Hooper, P. A. Melt pool temperature and cooling rates in laser powder bed fusion, Additive Manufacturing 2018, vol. 22, pp. 548–559, doi: 10.1016/j.addma.2018.05.032.
16. Vallabh C. and Zhao X. Melt pool temperature measurement and monitoring during laser powder bed fusion based additive manufacturing via single-camera two-wavelength imaging pyrometry (STWIP). Journal of Manufacturing Processes 2022, vol. 79, pp. 486–500, doi: 10.1016/j.jmapro.2022.04.058.
17. Blackbody Source Pegasus R. [online]. https://www.klasmeier.com/wp-content/uploads/2018/03/Datenblatt-Pegasus-R.pdf (Accessed April 11, 2023).

Preprints (www.preprints.org) | NOT PEER-REVIEWED | Posted: 28 April 2023 doi:10.20944/preprints202304.1158.v1

18. Shapiro, J. H.; Boyd, R. W. The physics of ghost imaging. Quantum Inf Process 2012, vol. 11, num. 4, pp. 949-993, doi: 10.1007/s11128-011-0356-5.